scientific reports

OPEN

Effect of Ni/Sn ratio on microstructure and properties of Cu-Ni-Sn-P alloy

Xiaokang Chen[1], Xiangpeng Xiao[1✉], Dawei Yuan[1✉], Jinshui Chen[2✉] & Yu Wu[3]

Cu-1.33Ni-1.35Sn-0.08P(Ni/Sn = 1/1), Cu-0.87Ni-1.82Sn-0.08P (Ni/Sn = 1/2) and Cu-1.78Ni-0.86Sn-0.08P (Ni/Sn = 2/1) alloys were prepared to explore the effect of different Ni/Sn ratios on the microstructure and properties of the alloys. The results showed that the alloy had the best properties when Ni/Sn = 1/2. At peak aging, its tensile strength and conductivity reached 447.3 MPa and 35.5% IACS respectively. Its tensile strength was 65.1 MPa and 88.8 MPa higher than that of the alloys with Ni/Sn = 1/1 and Ni/Sn = 2/1 respectively, and its conductivity was 1.1% IACS and 3.9% IACS higher. All three alloys had obvious dendrite segregation, but the alloy with Ni/Sn = 1/2 had finer dendrites and a more uniform distribution. In addition, the precipitates in the Cu-Ni-Sn-P alloys with Ni/Sn = 1/2 and Ni/Sn = 1/1 were all granular $Ni_{12}P_5$ phases, and the particles of the former are finer. The precipitates in the Cu-Ni-Sn-P alloy with Ni/Sn = 2/1 were rod-shaped. The strengthening mechanisms of the three alloys were Orowan strengthening, grain boundary strengthening, solid solution strengthening and dislocation strengthening, and Orowan strengthening was dominant. The Cu-Ni-Sn-P alloy with Ni/Sn = 1/2 had finer grains and precipitates, resulting in better tensile strength and electrical conductivity.

Keywords Cu-Ni-Sn-P alloy, Tensile strength, Dendrite segregation, $Ni_{12}P_5$ phases, Orowan strengthening

In order to meet the requirements of high density assembly of integrated circuit products, integrated circuit packaging lead frame is developing towards the high density direction characterized by high integration, high performance, multiple leads and narrow spacing. As the alloy material encapsulated in integrated circuit, it will generate heat in the working process, and the working temperature is sometimes high. Therefore, it is required that the alloy can still maintain stable performance and have good thermal stability under high temperature treatment. At present, the main brands of lead frame materials on the market are C19400(Cu-Fe-P) alloy, C18150(Cu-Cr-Zr) alloy and C70250(Cu-Ni-Si) alloy.

As a new lead frame material, Cu-Ni-Sn-P alloy has the advantages of low cost, good processing performance, simple production process and excellent comprehensive performance, which can meet the market demand of middle and high-end lead frames. However, the addition of Sn element will lead to segregation behavior of the alloy[1–4], resulting in coarse dendrites, which is not conducive to obtaining better properties and property stability of the alloy. In addition, the solid solution of Ni element has a great influence on the conductivity of the alloy[5–7]. Therefore, reducing dendrite segregation and refining dendrite are the key factors to prepare high performance Cu-Ni-Sn alloys. Researchers improve the structure and properties of Cu-Ni-Sn alloy by microalloying[8–10]. Wang[9] studied the effect of Ti addition on the microstructure and tensile strength of Cu-Ni-Sn alloy and found that Ti can effectively improve the tensile strength of the alloy and optimize the alloy microstructure. Empl[11] studied the effects of Al, Mn, Zr, B or P elements on the high temperature mechanical properties of Cu-Ni-Sn-Pb alloys, and found that B or P can significantly improve the high temperature mechanical properties of the alloys. The reason is attributed to the combination of capillary pinning and the mechanical shielding of these particles to molten lead inclusions in the alloy. Zhang[12] showed in the study of low-content Cu-Ni-Sn-P alloy that the alloy had multiple strengthened characteristics of solid solution strengthening, precipitation-hardening and work hardening. Hu[13] found in the study of Cu-Ni-P that slate-like Ni_2P phase would be generated during aging precipitation, which has a strengthening effect on the alloy. Guo[14] found intermetallic compounds containing P formed at grain boundaries by adding 0.1wt.% P to Cu-Ni-Sn, and nailed grain boundaries to refine grains. F, Nishijima[8] found that when Sn element is added to Cu-Ni-P, under the compound addition of Ni and P, the

[1]Jiangxi Advanced Copper Industry Research Institute, JiangXi University of Science and Technology, Yingtan 335000, China. [2]School of Materials Science and Engineering, JiangXi University of Science and Technology, Ganzhou 341000, China. [3]Institute of Applied Physics, Jiangxi Academy of Sciences, Nanchang 330096, China. ✉email: xiao_xiangpeng@126.com; 1458229619@qq.com; chenjinshui0797@163.com

segregation can form A Koch air mass around the dislocation and hinder the dislocation movement. P can effectively improve the microstructure and comprehensive properties of the alloy, but it still fails to solve the problem of dendrite coarseness. In this paper, authors propose to optimize the dendrite segregation by adjusting the Ni/Sn ratio, thus improving the tensile strength and electrical conductivity of the alloy. Subsequently, the authors studied the effect of aging on the microstructure (the size and composition of precipitates), and discussed the microscopic mechanism, which provided a reference for the subsequent production research.

Therefore, three different Cu-Ni-Sn-P alloys with Ni/Sn ratio of 1/1, 1/2 and 2/1 were designed in this paper. The effects of different Ni/Sn ratios on the microstructure and properties of Cu-Ni-Sn-P alloys were systematically analyzed.

Experimental materials and methods

Electrical copper rod, Cu-57wt.% Ni master alloy, pure tin particles and Cu-14wt.% P master alloy were used as raw materials. The vacuum induction melting equipment was used to melt and cast the material under the protection of an argon atmosphere. The chemical compositions of the three alloys were Cu-1.33Ni-1.35Sn-0.08P, Cu-0.87Ni-1.82Sn-0.08P, and Cu-1.78Ni-0.86Sn-0.08P alloys, respectively. The three alloys were sized at 150 mm×150 mm×32 mm after the ingot was cast. The composition of the Cu-Ni-Sn-P alloy ingot was detected by an inductively coupled plasma (ICP) emission spectrometer. The total mass fraction of Ni and Sn was controlled at about 2.7 wt% and the Ni/Sn ratio was 1/1, 1/2 and 2/1 respectively. The mass fraction of P was stably controlled at 0.07 wt%-0.08 wt%. The ingots were successively hot-rolled, solution treated and aged.

After the alloy ingot had been turned and milled, the shrinkage tail was removed. The ingot was then hot rolled, and following this, the sample that had undergone hot rolling was subjected to solution treatment at 850 °C for 60 min. Subsequently, the aging temperature and time were explored. At the same time, the effect of pre-cooling deformation on the microstructure and properties is investigated.

The samples were rolled by Wuxi lianxing φ 320*500 two-roll mill, and heat treated by Shanghai Shiyan SX2-5-12 box-type resistance furnace. Microvickers hardness tester (Huayin 200HVS-5) and digital eddy current metal conductance tester (Sigma2008B/C) were used to measure hardness and conductivity. The microstructure and morphology of the alloy were analyzed by Zeiss Axioskop 2 MAT optical microscope, FEI MLA 650 F field emission scanning electron microscope and energy dispersive spectrometer, and TECNAI G2-20 transmission electron microscope. The transmission sample was prepared by electrolysis with a double spray solution of 25% nitric acid + 75% methanol (volume fraction) at a temperature of -30 °C.

Results

Performance evolution analysis

Figure 1 shows vickers hardness and conductivity of the Cu-Ni-Sn-P alloys with different Ni/Sn ratios. The alloy with Ni/Sn ratio of 1/2 has higher hardness in as cast and solid solution state (Fig. 1a). The hardness of as cast alloy with Ni/Sn = 1/2 is 66 HV, which is 3.9 HV and 2.8 HV higher than that of alloy with Ni/Sn = 1/1 and Ni/Sn = 2/1, respectively. The as cast alloy with Ni/Sn = 1/2 has a higher hardness, and its conductivity is slightly lower than that of the alloy with Ni/Sn = 1/1, but higher than that of the alloy with Ni/Sn = 2/1. The conductivity of the alloy with Ni/Sn = 1/2 in the solid solution state is higher than that of the other two alloys. It should be noted that the vickers hardness and conductivity of the three alloys decreased after solution treatment. The decrease in hardness is attributed to the softening of the alloy, while the decrease in conductivity is attributed to the increasing in electron scattering due to the dissolution of the primary phase[15].

Figure 2 shows the change curve of mechanical properties and electrical conductivity of three alloys with aging time. It is obvious that the tensile strength and vickers hardness of the three alloys increase rapidly at first and then decrease slowly with the increase of aging time (Fig. 2a,b). In generally, at the beginning of aging, a large number of precipitated phases precipitate from the Cu matrix, resulting in an increase in the strength of the alloy. With the increase of time, the Cu matrix recrystallizes and the precipitates coarsen, leading to the decrease of alloy strength. It is different that the tensile strength of alloy with Ni/Sn = 1/2 is higher than that of alloy with
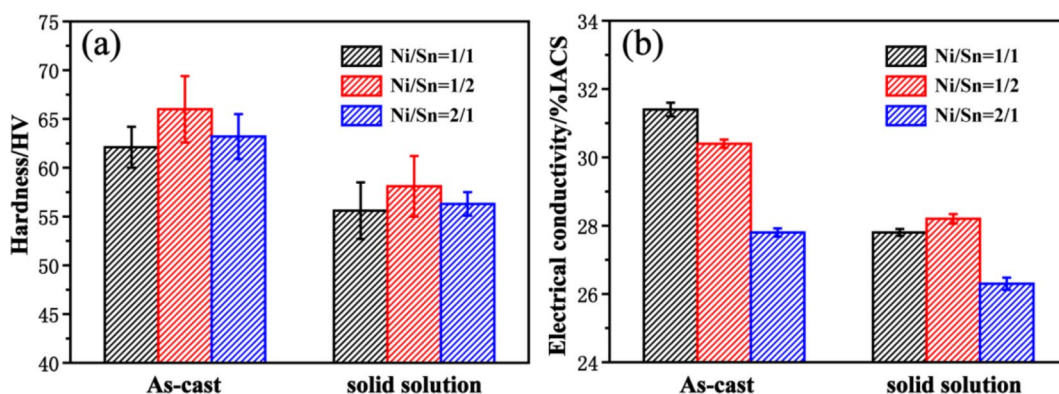

Fig. 1. Properties of the three Cu-Ni-Sn-P alloys in as-cast and solid solution state (**a**) hardness; (**b**) electrical conductivity.
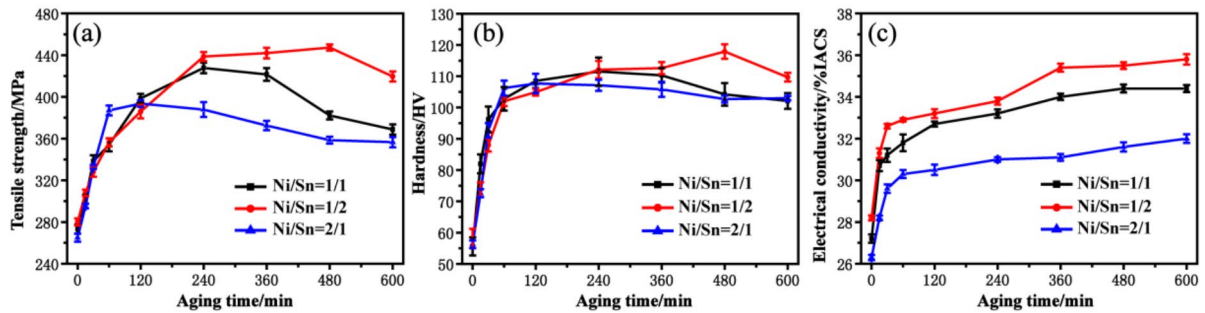
Fig. 2. Mechanical and electrical properties of three Cu-Ni-Sn-P alloys after isothermal aging at 450 °C, (**a**) Tensile strength, (**b**) Hardness, (**c**) Electrical conductivity.
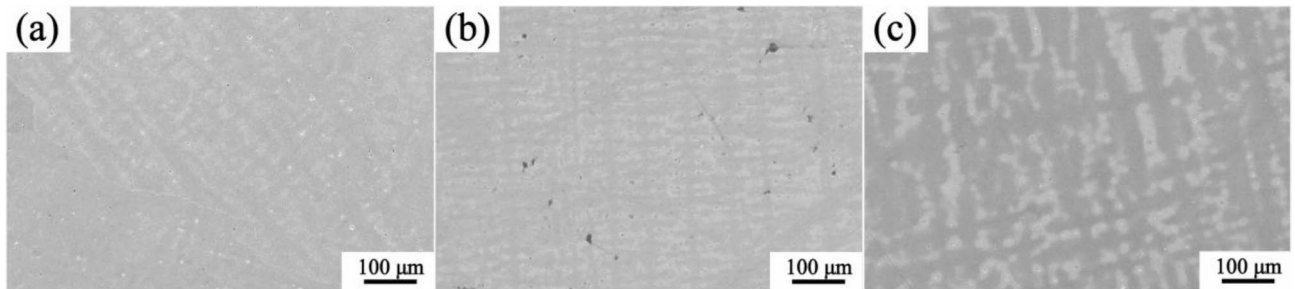

Fig. 3. SEM Microstructure of as-cast Cu-Ni-Sn-P alloys. (**a**) Ni/Sn = 1/1, (**b**) Ni/Sn = 1/2, (**c**) Ni/Sn = 2/1.

Ni/Sn = 1/1 and Ni/Sn = 2/1. Its strength reaches 447.3 MPa, which is 65.1 MPa and 88.8 MPa higher than that of the alloys with Ni/Sn = 1/1 and Ni/Sn = 2/1 after aging at 450 °C for 480 min. The decrease of tensile strength is smaller, indicating that the alloy with Ni/Sn = 1/2 has higher softening resistance. In addition, the three alloys have good thermal stability, and the strength and hardness of the alloy have no obvious attenuation with the increase of aging time. The thermal stability of Cu-Ni-Sn-P alloy with Ni/Sn = 1/2 is more excellent, and it can still maintain high tensile strength and hardness after aging for 600 min.

The conductivity of the three alloys increase rapidly at first and then slowly with the increase of aging time. The supersaturated solid solution precipitates from the Cu matrix during aging, which greatly reduces the scattering effect of solid solution atoms on electrons. At the beginning of aging, the alloy has a greater driving force for precipitation. The driving force decreases with the precipitation of solid solution atoms, resulting in a slower increase in the alloy conductivity. It is worth noting that the conductivity of the alloy with Ni/Sn = 1/2 is higher than that of the other two alloys. Its conductivity reaches 35.5% IACS, which is 1.1% IACS and 3.9% IACS higher than that of the alloy with Ni/Sn = 1/1 and Ni/Sn = 2/1 respectively.

Microstructural evolution analysis

Figure 3 shows the SEM microstructures of the as-cast Cu-Ni-Sn-P alloys with different Ni/Sn ratios. It is obvious that there is a certain degree of dendritic segregation in the three alloys. The dendrite segregation of the alloy with Ni/Sn = 1/1 is coarser, and the dendrite arm spacing is larger. It is closely related to the content of Sn element, and the dendrites of the alloy become coarser with the increasing of Sn addition. However, the dendrite and dendrite arm of the alloy with Ni/Sn = 1/2 are smaller than those of the other two alloys, and their distribution is more uniform. The composition difference between solid and liquid phases increases with the decrease of Ni/Sn ratio (the increase of Sn content), which leads to the increase of the component supercooling tendency and the nucleation rate of the second phase[16]. And the growth of dendrites is mutually inhibited during solidification, resulting in finer and more uniform dendrites.

To determine the composition of dendrite phase, EDS surface scanning analysis was carried out for the three alloys, as shown in Fig. 4. It is obvious that the dendrites of the three alloys are composed of black and gray contrast. The black contrast part contains Ni, Sn and P elements, while the gray contrast part is mainly caused by the enrichment of Sn elements. In order to further determine the element content of dendrites with different contrast, EDS point scanning analysis was carried out for the alloy with Ni/Sn = 1/2, as shown in Table 1. The contents of Ni, Sn and P in the black contrast (EDS1) phase are 1.51 wt,%, 0.85 wt,% and 11.89 wt,% respectively. The contents of Ni and P in gray and matrix phases are relatively low, mainly including Sn and Cu, which are consistent with the EDS scanning results.

Figure 5 shows the SEM microstructures of the solid solution Cu-Ni-Sn-P alloys with different Ni/Sn ratios. It is obvious that the dendritic phases in the three alloys are all solid solution into the Cu matrix, which is the
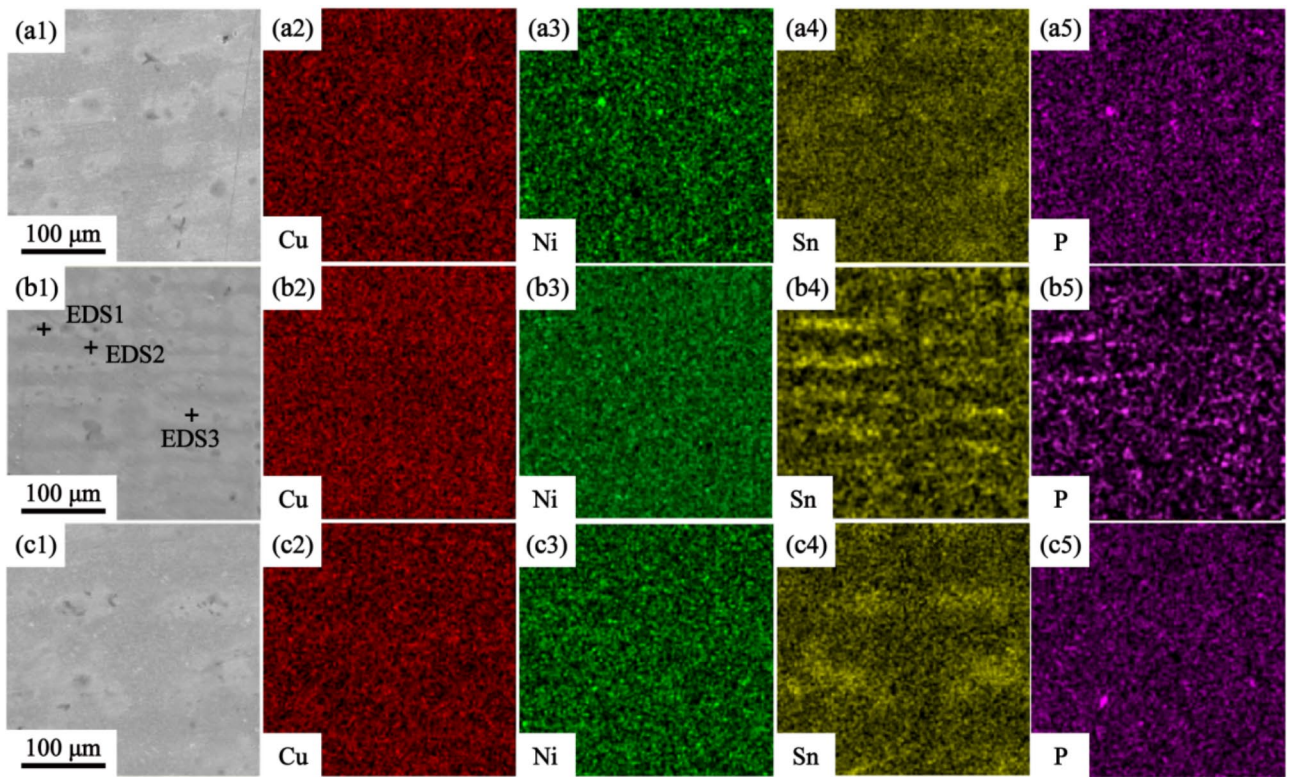
Fig. 4. EDS scanning results of as-cast Cu-Ni-Sn-P alloy. (**a1-a5**) Ni/Sn = 1/1, (**b1-b5**) Ni/Sn = 1/2,(**c1-c5**) Ni/Sn = 2/1.

Location	Ni	Sn	P	Cu
EDS1	1.51	0.85	11.89	85.87
EDS2	0.50	0.33	0.00	99.17
EDS3	0.74	6.01	0.09	93.16

Table 1. EDS point scan results(wt,%).
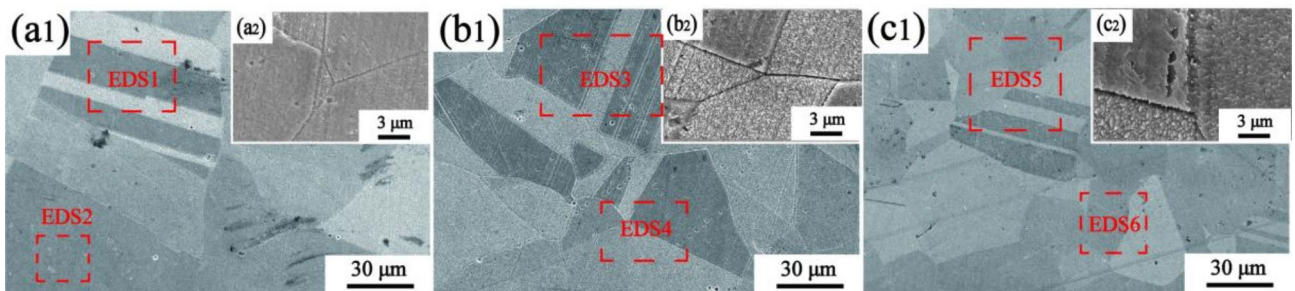
Fig. 5. SEM microstructure of solid solution Cu-Ni-Sn-P alloys. (**a**) Ni/Sn=1/1,(**b**) Ni/Sn=1/2,(**c**) Ni/Sn=2/1.

main reason for the decrease of conductivity after solution treatment. There are a lot of recrystallized grains and twins in the alloy. The solution treatment eliminated some dislocations in the alloy, and reduced the second phase in the matrix, leading to the reduction of the mechanical properties of the alloy. It can be found that the content of Ni, Sn and P in the alloy is consistent with the actual addition amount through the area scanning of three alloys (Table 2).

Figure 6 shows the microstructure of under aged, peak aged and over aged Cu-Ni-Sn-P alloys with different Ni/Sn ratios at 450 ºC. These three alloys have many twins and second phases after aging, and the grain size of

Alloy	Location	Ni	Sn	P	Cu
Cu-1.33Ni-1.35Sn-0.08P	EDS1	1.24	1.30	0.07	Bal.
	EDS2	1.32	1.35	0.09	Bal.
Cu-0.87Ni-1.82Sn-0.07P	EDS3	0.79	1.82	0.07	Bal.
	EDS4	0.88	1.79	0.07	Bal.
Cu-1.78Ni-0.86Sn-0.07P	EDS5	1.82	0.92	0.06	Bal.
	EDS6	1.89	0.85	0.08	Bal.

Table 2. Area surface scanning results of three alloys (*wt*%).
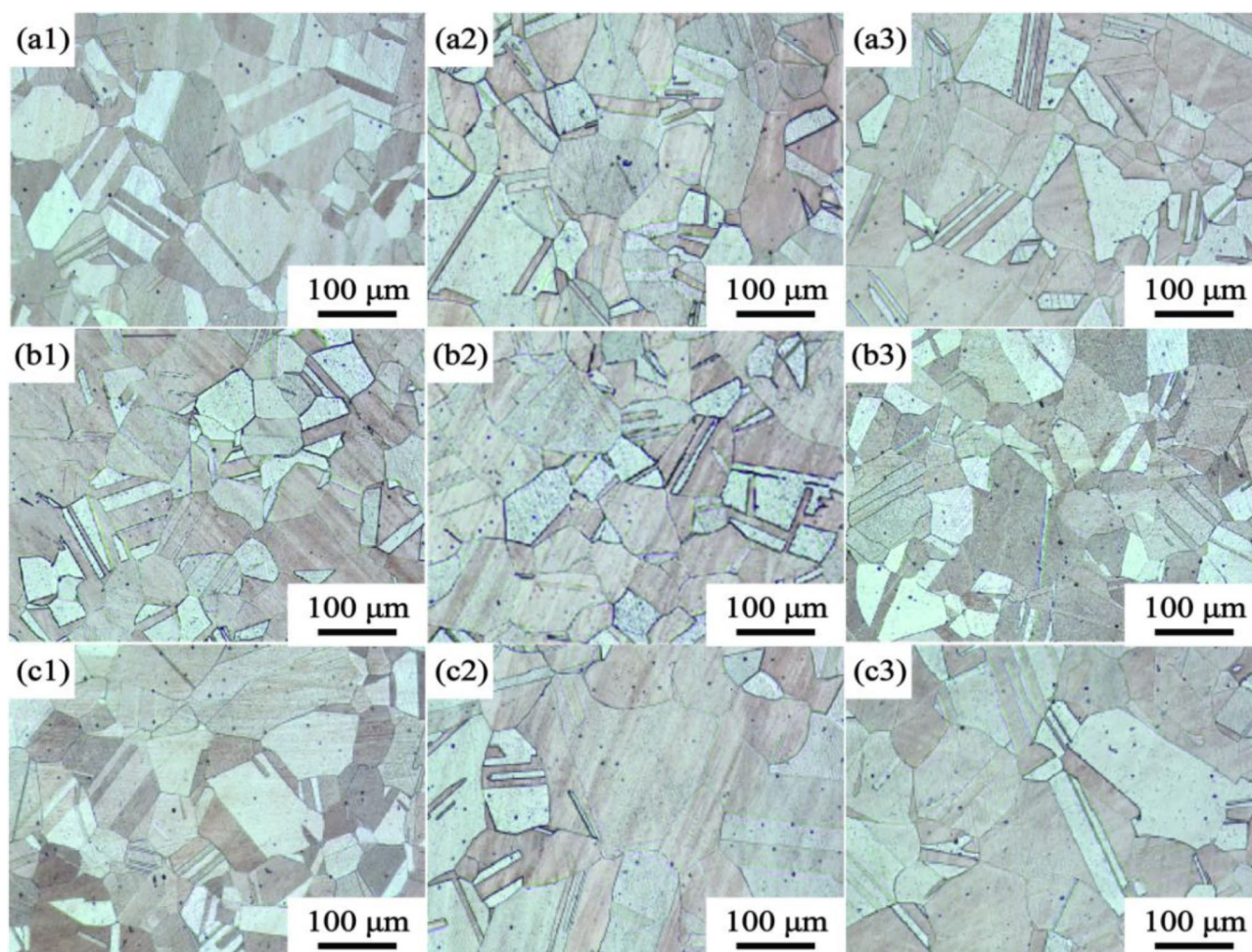
Fig. 6. The microstructure of under aged, peak aged and over aged Cu-Ni-Sn-P alloys at 450 °C, (**a1-a3**) Ni/Sn = 1/1, (**b1-b3**) Ni/Sn = 1/2[16],(**c1-c3**) Ni/Sn = 2/1, (**a1**) (**b1**) (**c1**) under aged, (**a2**) (**b2**) (**c2**) peak aged, (**a2**) (**b2**) (**c2**) over aged.

under aging, peak aging and over aging has no significant difference. Figure 6 shows that the grain morphology of the alloy containing Ni/Sn = 1/2 is slightly smaller than the other two alloys.

Figure 7 shows the SEM microstructure of the peak aged Cu-Ni-Sn-P alloys with different Ni/Sn ratios at 450 °C. A large number of coarse grains exist in Cu-Ni-Sn-P alloys with different Ni/Sn ratios, which is consistent with the results shown in Fig. 6. Fine precipitates with diameters ranging from 100 nm to 600 nm were found in the crystals.

Figure 8 shows the SEM microstructure of peak aged Cu-Ni-Sn-P alloy fractures with different Ni/Sn ratios at 450 °C. It is obvious that the dimple of the Cu-Ni-S-P alloy with Ni/Sn = 1/2 is more uniform than that of the Cu-Ni-Sn-P with Ni/Sn = 1/1 and Ni/Sn = 2/1. There are many tongue like patterns and quasi cleavage dimples on the fracture surface of the Cu-Ni-Sn-P alloy with Ni/Sn = 2/1, which indicates that there are many large particle hard spots in the crystal. In addition, tongue pattern and quasi cleavage dimple of the Cu-Ni-Sn-P alloy with Ni/
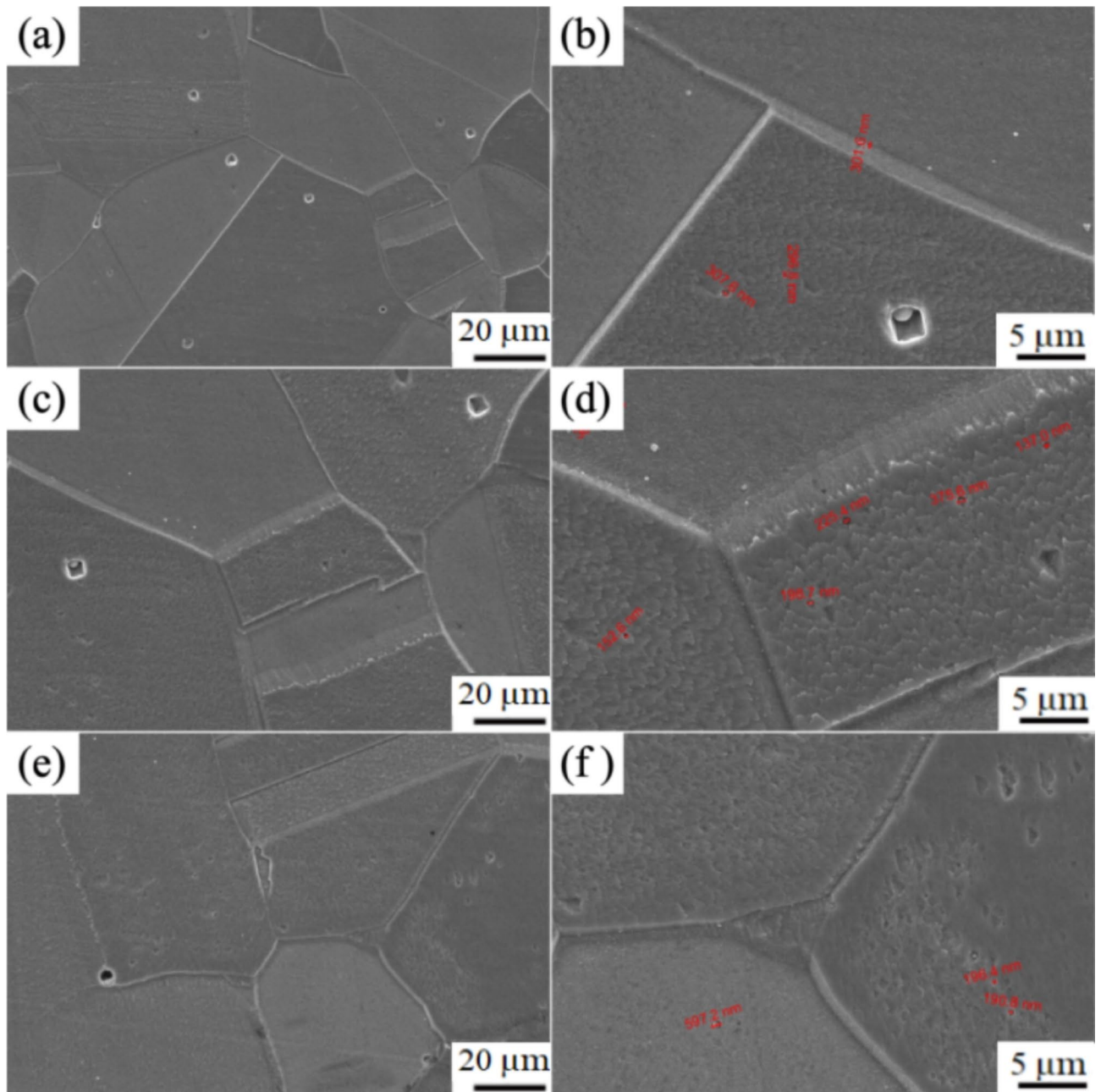
Fig. 7. The SEM microstructure of peak aged Cu-Ni-Sn-P alloys with different Ni/Sn ratios at 450 ℃, (**a, b**) Ni/Sn = 1/1,(**c** , **d**) Ni/Sn = 1/2[16],(**e, f**) Ni/Sn = 2/1.

Sn = 1/1 are relatively few. The fracture surface of the Cu-Ni-Sn-P alloy with Ni/Sn = 1/2 is dimple distribution, indicating that its plasticity is more excellent.

To further analyze the appearance and distribution of the second phase in the alloy, TEM microstructure was observed, as shown in Fig. 9. It is obvious that a certain amount of precipitates appear in the three alloys. It is different that the precipitates in Cu-Ni-Sn-P alloys with Ni/Sn = 1/1 and Ni/Sn = 1/2 are spherical and the particles of the latter are finer and denser, its strength is better, while those in Cu-Ni-Sn-P alloy with Ni/Sn = 2/1 are rod like. The precipitation phase in Cu-Ni-Sn-P alloy is finer with the increase of Sn content, indicating that Sn plays a leading role in the morphology of precipitation phase. It can be found from SADP that the precipitates in Cu-Ni-Sn-P alloys with Ni/Sn = 1/1 and Ni/Sn = 1/2 are $Ni_{12}P_5$ phase (Figs. 9(a2), (b2)).

Discussion
Effect of different Ni/Sn ratio on microstructure of the Cu-Ni-Sn-P alloy
Segregation of Sn element is the key factor affecting the properties of Cu-Ni-Sn-P alloy. Ni element mainly plays the role of solution strengthening in Cu alloy. However, Ni element has a great influence on the conductivity
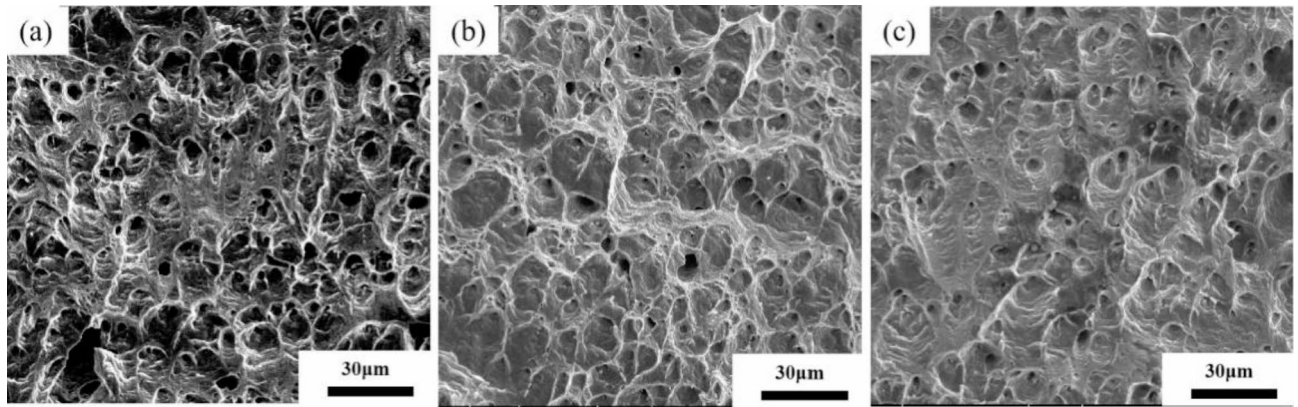
Fig. 8. The SEM microstructure of peak aged Cu-Ni-Sn-P alloy fractures with different Ni/Sn ratios at 450 ºC, (**a**) Ni/Sn = 1/1,(**b**) Ni/Sn = 1/2,(**c**) Ni/Sn = 2/1.

of the alloy. Therefore, in order to reduce the solid solubility of Ni and inhibit the growth of Sn dendrites, the second phase distribution is optimized by adjusting the Ni/Sn ratio and adding P. The Cu-Ni-Sn-P alloys with different Ni/Sn ratios occurred dendrite segregation, the dendrites of Ni/Sn = 1/2 alloy are finer and more uniform. The concentration of dendrite crystallization front is higher and the component undercooling is increased during the solidification process. The concentration of dendrite crystallization front is higher and the component undercooling is increased during the solidification process. The decrease of Ni/Sn ratio leads to the continuous increase of composition difference between solid phase and liquid phase, which leads to the increase of constitutional supercooling and nucleation rate[17]. The interdendritic growth of the two dendrites inhibits each other, resulting in the smaller dendrites. There are a large number of second phase precipitates in the three alloys during aging, and the particles of precipitates in Cu-Ni-Sn-P alloy with Ni/Sn = 1/2 are finer, more dense, and more evenly distributed. On the one hand, the content of Ni element in Cu-Ni-Sn-P alloy with Ni/Sn = 1/2 is less, which is unfavorable to the growth of precipitation phase; on the other hand, Sn element inhibits the coarsening of $Ni_{12}P_5$ phase. The finer precipitates are more beneficial for pinning dislocations and inhibiting their movement, leading to better mechanical properties of Cu-Ni-Sn-P alloy. It is also the main reason that the fracture morphology is uniform dimple.

Strength increment calculation of Cu-Ni-Sn-P alloy during aging

The strengthening modes of the Cu-Ni-Sn-P alloy are mainly solution strengthening, grain boundary strengthening and Orowin strengthening. Therefore, the strength of peak aged Cu-Ni-Sn-P alloy Ni/Sn = 1/1, Ni/Sn = 1/2 and Ni/Sn = 1/1 is calculated to explore the influence of different Ni/Sn ratios on the strength contribution of the alloy.

Orowan reinforcement

The yield strength increment of Orowan strengthening is the result of the interaction between dislocation and nanoparticles, which can be expressed as[1,18]:

$$\Delta \sigma_{Orowan} = \frac{0.81MGb}{2\pi(1-\nu)^{1/2}} \frac{ln(d_{precip}/b)}{\lambda - d_{precip}} \quad (1)$$

$$\lambda = \frac{d}{2}(\frac{3\pi}{2f_{precip}})^{1/2} \quad (2)$$

where G = 46 GPa is the shear modulus of matrix and d_{precip} is the diameter of precipitated phase, which can be measured by the microscopic morphology. $\nu = 0.34$ is Poisson's ratio, and $b = 0.2556$ nm is Burgers vector. f_{precip} is the volume fraction of particles and λ is the average plane spacing between precipitated phases. The values of G, ν and b do not change for the same material. The diameters of precipitated phase of the Cu-Ni-Sn-P alloy with Ni/Sn=1/1, Ni/Sn = 1/2 and Ni/Sn=2/1 are 6.4 nm, 3.9 nm and 7.5 nm, respectively. The volume fractions of precipitated phase are 0.83, 0.79 and 0.61%, respectively.

Grain boundary strengthening

The effect of grain boundary strengthening on yield strength increment is usually calculated by the Hall-Petch equation[19]:

$$\Delta \sigma_{GB} = \frac{K_y}{\sqrt{d_G}} \quad (3)$$

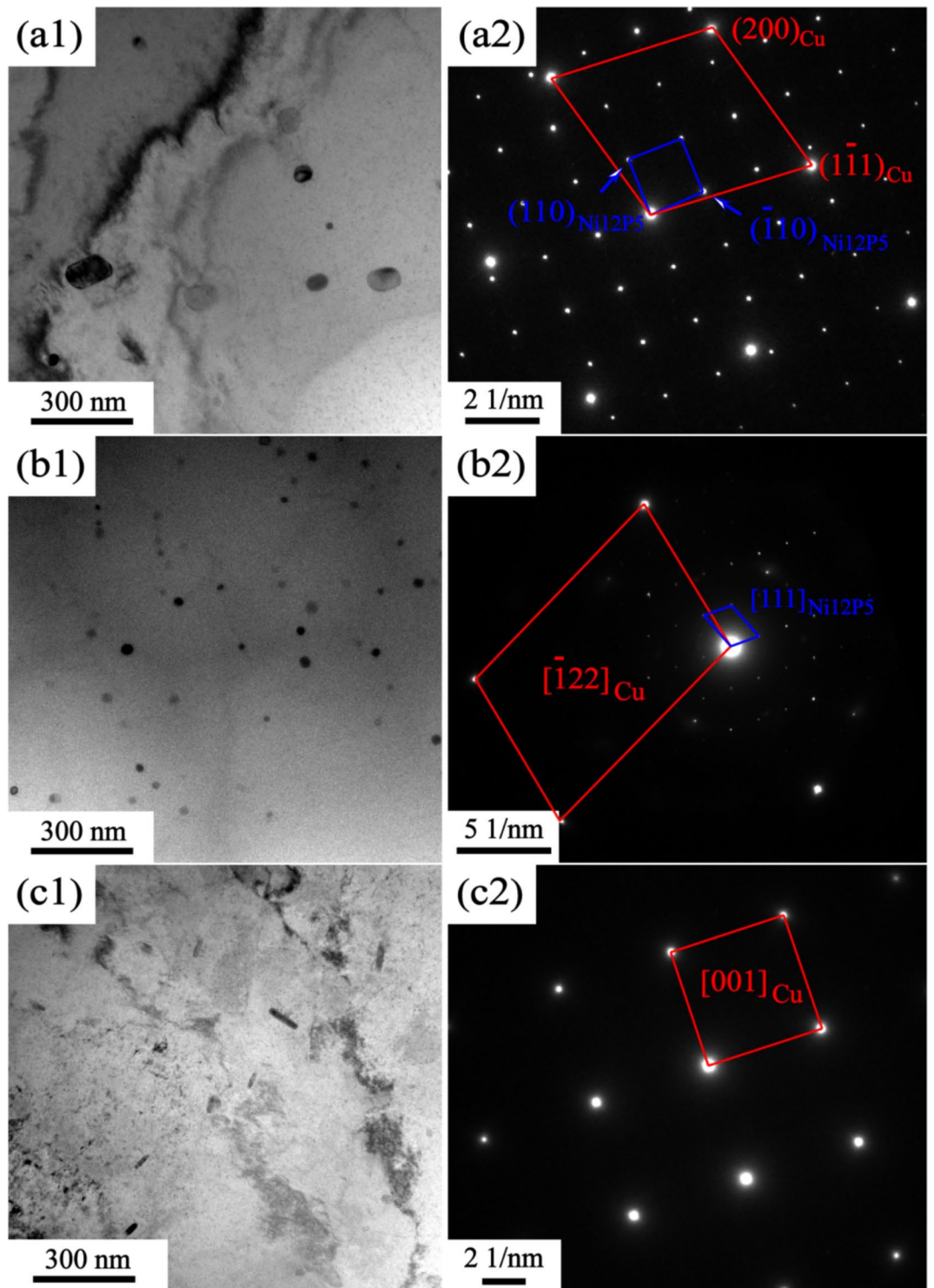where d_G is grain diameter and $K_y = 0.15$ is constant.

Fig. 9. The TEM microstructure of peak aged Cu-Ni-Sn-P alloy fractures with different Ni/Sn ratios at 450 °C, (**a1**,**a2**) Ni/Sn = 1/1,(**b1, b2**) Ni/Sn = 1/2,(**c1, c2**) Ni/Sn = 2/1, (**a2**) (**b2**) (**c2**) SADP.

Solid solution strengthening

$\Delta \sigma_{Solid\ solution}$ represents the influence of alloying elements in the matrix, The increment of yield strength due to lattice distortion caused by solute atoms in copper matrix is called solid solution strengthening, Expressed by formula (4)[20]:

$$\Delta \sigma_{Solid\ solution} = G(|\delta| + \frac{1}{20})|\eta|^{\frac{3}{2}}\sqrt{\frac{x_{\alpha}}{3}} \tag{4}$$

alloys	Dislocation density ρ/m^{-2}
Ni/Sn = 1/1	7.44×10^{12}
Ni/Sn = 1/2	1.41×10^{13}
Ni/Sn = 2/1	6.29×10^{12}

Table 3. Dislocation density of Cu-Ni-Sn-P alloy.

alloys	$\Delta \sigma_d$	$\Delta \sigma_{Ss}$	$\Delta \sigma_{GB}$	$\Delta \sigma_{Orowan}$
Ni/Sn = 1/1	106.3	96.1	84.8	134.3
Ni/Sn = 1/2	102.4	94.9	97.3	141.7
Ni/Sn = 2/1	100.2	102.7	72.8	117.0

Table 4. Calculation results of strength increment of alloy /MPa.

Where, G is the shear modulus of matrix, $\delta = 0.1105$ is the factor of lattice change, $\eta = 0.3171$ is a factor to describe the change of shear modulus caused by alloying, and x_α is the atomic content of solute in solid solution. Ni is the main strengthening element in solid solution measured by energy spectrum.

Dislocation strengthening
The contribution of $\Delta \sigma_d$ reaction dislocation density to yield strength, the work hardening is realized by dislocation increase, which increases the strength. The increment of yield strength can be calculated by Taylor equation. The dislocation density is calculated by using XRD diffraction pattern and formula (5) proposed by Williamson et al.[21] The dislocation density in the alloy structure was obtained, and the results were shown in Table 3.

$$\Delta \sigma_d = M \alpha G b \rho^{\frac{1}{2}} \tag{5}$$

Where, α = 0.26 is FCC metal constant, dislocation density, M = 3.06 is Taylor factor, G is shear modulus, and B is Burgers vector[22,23].

$$\rho = 2\sqrt{3} \cdot \epsilon / (D \cdot b) \tag{6}$$

where ε is the microscopic strain, D is the grain size, and b is the Burgundy vector (for FCC Cu-Ni-Sn-P alloy, $b = \left(\sqrt{2}/2\right) a$. Both ε and D can be calculated by formula (7) from a linear fitting parameter of diffraction Angle and half peak width in X-ray diffraction results of samples.

$$\beta \cdot cos\theta = K\lambda / D + (4 sin\theta) \epsilon \tag{7}$$

where β is the half-peak width, θ is the Bragg Angle of a peak, K is a constant (~ 0.9), λ = 0.15405 nm is the wavelength of CuKα radiation.

As shown in Table 4, is the incremental contribution of different strengthening methods to the yield strength of the alloy. According to the data in the table, the main strengthening method of Cu-Ni-Sn-P alloy is Orowan strengthening, which is consistent with the experimental results. When Ni/Sn = 1/2, the spherical bore-centered tetragonal $Ni_{12}P_5$ phase is more dispersed in the matrix. The grain boundary strength increment of $\Delta \sigma_{GB}$ is the highest among the three, indicating that when Ni content decreases and Sn content increases, the microstructure refinement improves the alloy strength. The combined effect of the two significantly improves the strength of the alloy. At the same time, with the increase of Sn content, dislocation density increases, which is related to the formation of Colloid air mass by Sn in the matrix[15]. Colloid air mass has increased viscous resistance to dislocation movement, contributing to the improvement of alloy strength.

Conclusion
(1) When the total content of Ni and Sn is constant, the microstructure and properties of Cu-Ni-Sn-P alloy can be effectively improved by adjusting the Ni/Sn ratio. It provides a theoretical basis for the optimization of Cu-Ni-Sn-P alloy composition. The tensile strength and electrical conductivity of Cu-Ni-Sn-P alloy with Ni/Sn = 1/2 are higher than those of alloys with Ni/Sn = 1/1 and Ni/Sn = 2/1. The tensile strength and conductivity of the Cu-Ni-Sn-P alloy with Ni/Sn = 1/2 reached 447.3 MPa and 35.5% IACS respectively. Its tensile strength was 65.1 MPa and 88.8 MPa higher than that of the alloys with Ni/Sn = 1/1 and Ni/Sn = 2/1 respectively, and its conductivity was 1.1% IACS and 3.9% IACS higher.

(2) When the ratio of Ni to Sn is 1/2, the microstructure of Cu-Ni-Sn-P alloy is significantly optimized, the dendrite is optimized and the nano precipitates ($Ni_{12}P_5$ phases) are refined, which is the main reason for its higher strength. In addition, The strengthening models of the three alloys are Orowan strengthening, grain boundary strengthening, dislocation strengthening and grain boundary strengthening.

Data availability

All the necessary data are included in the manuscript. Any additional data can be made available upon request. If anyone requests data for this study, please contact us .

References

1. Li, J. et al. Effect of Cr and Sn additions on microstructure, mechanical-electrical properties and softening resistance of Cu-Cr-Sn alloy. *Mater. Sci. Eng. A.* **802**, 140628 (2021).
2. Miettinen, J. Thermodynamic description of the Cu-Ni-Sn system at the Cu-Ni side. *Calphad* **27**, 309–318 (2003).
3. Zielińska, M. Wnuk. Microstructural and thermal analysis of Cu-Ni-Sn-Zn alloys by means of SEM and DSC techniques. *Arch. Mater. Sci. Eng.* **40**, (2009).
4. Kratochvíl, P., Mencl, J., Pešička, J. & Komnik, S. The structure and low temperature strength of the age hardened Cu-Ni-Sn alloys. *Acta Metall.* **32**, 1493–1497 (1984).
5. Liu, J. et al. The effect of cold rolling on age hardening of Cu-3Ti-3Ni-0.5Si alloy. *J. Alloys Compd.* **797**, 370–379 (2019).
6. Butler, E. & Thomas, G. Structure and properties of spinodally decomposed Cu-Ni-Fe alloys. *Acta Metall.* **18**, 347–365 (1970).
7. Zhao, D. et al. Structure and strength of the age hardened Cu-Ni-Si alloy. *Mater. Chem. Phys.* **79**, 81–86 (2003).
8. Nishijima, F., Nomura, K., Watanabe, C. & Monzen, R. Investigation on stress relaxation behavior in Cu-Ni-Sn-P alloys. *J. Jpn Inst. Met.* **72**, 427–432 (2008).
9. Wang, Y. et al. Influence of Ti on microstructure and strength of c-BN/ Cu-Ni-Sn-Ti composites. *Int. J. Refract. Met. Hard Mater.* **29**, 293–297 (2010).
10. Liu, F. et al. Study on softening resistance performance of Cu-Sn-Ni-P alloy for lead frame. *Hot Work Technol.* **45**, 63–66 (2016).
11. Empl, D. et al. Improvement of elevated temperature mechanical properties of Cu-Ni-Sn-Pb alloys. *Mater. Sci. Eng.* **527**, 4326–4333 (2010).
12. Zhang, W. et al. Research on heat resistance of Cu-Ni-Sn-P alloy. *Copp. Eng.* **3**, 12–15 (2019).
13. Hu, T. et al. On the morphology and crystallography of the strengthening precipitates in an aged Cu-Ni-P alloy. *J. Alloys Compd.* **729**, 84–88 (2017).
14. Guo, C. et al. Effects of P addition on spinodal decomposition and discontinuous precipitation in Cu-15Ni-8Sn alloy. *Mater. Charact.* **171**, 110760 (2020).
15. Jie, X. et al. Effect of Sn addition on high temperature softening resistance of Cu-3Ni-0.75Si-0.1Mg alloy and its mechanism. *Trans. Mater. Heat. Treat.* **42**, 32–42 (2021).
16. Xiong, S. et al. Microstructure and properties of microalloyed Cu-Ni-Sn-P alloy. *Heat. Treat. Met.* **47**, 164–170 (2022).
17. Zhao, J. et al. Nanocrystalline Cu-Ni-Sn-P alloy was prepared by amorphous crystallization method. *Chin. Sci. Bull.* **39**, 1581–1583 (1994).
18. Gao, H., Wang, J., Da, S. & Sun, B. Microstructure and properties of Cu–11Fe–6Ag in situ composite after thermo-mechanical treatments. *J. Alloys Compd.* **438**, 268–273 (2007).
19. Orowan, E. et al. Fracture and strength of solids. *Rep. Prog Phys.* **12**, 185–232 (1949).
20. Filgueira, M. & Pinatti, D. Situ diamond wires: part I. The Cu-15 vol.% nb high strength cable. *J. Mater. Process. Technol.* **128**, 191–195 (2002).
21. He, J. et al. A precipitation-hardened high-entropy alloy with outstanding tensile properties. *Acta Mater.* **102**, 187–196 (2016).
22. Liao, X., Zhao, Y. & Jin, Z. Microstructures and mechanical properties of ultrafine grained 7075 Al alloy processed by ECAP and their evolutions during annealing. *Acta Mater.* **52**, 4589–4599 (2004).
23. Cheng, H. et al. Controllable fabrication of a carbide-containing FeCoCrNiMn high-entropy alloy: microstructure and mechanical properties. *Mater. Sci. Technol.* **33**, 2032–2039 (2017).

Acknowledgements

Author contributions

Xiaokang Chen: Investigation, Experimental design, Methodology, Writing – original draft. Xiangpeng Xiao: Conceptualization, Supervision, Writing – review & editing. Dawei Yuan: Investigation, Formal analysis. Jinshui Chen: Formal analysis, Writing – review & editing. Yu Wu: Writing – review & editing.

Declarations

Competing interests

The authors declare no competing interests.

Additional information

Correspondence and requests for materials should be addressed to X.X., D.Y. or J.C.

Reprints and permissions information is available at www.nature.com/reprints.

Publisher's note Springer Nature remains neutral with regard to jurisdictional claims in published maps and institutional affiliations.